Controlled Nucleation and Growth of Pillared Paddlewheel Framework Nanostacks onto Chemically Modified Surfaces

Dara Van Gough,[†] Timothy N. Lambert,[†] David R. Wheeler,[†] Mark A. Rodriguez,[†] Michael T. Brumbach,[†] Mark D. Allendorf,[‡] and Erik D. Spoerke*,[†]
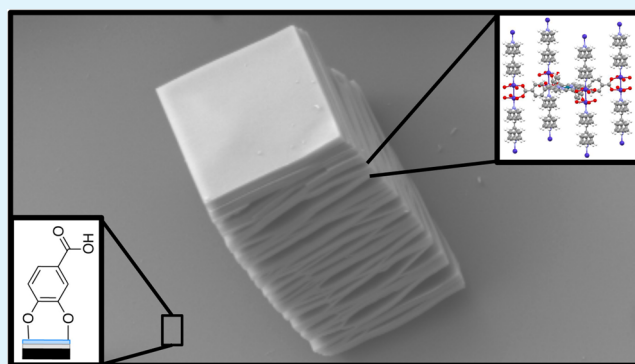
[†]Sandia National Laboratories, Albuquerque, New Mexico 87185, United States
[‡]Sandia National Laboratories, Livermore, California 94551, United States

ⓢ *Supporting Information*

ABSTRACT: The nucleation and growth of metal−organic frameworks onto functional surfaces stands to facilitate the utility of these supramolecular crystalline materials across a wide range of applications. Here, we demonstrate the solvothermal nucleation and growth of a pillared paddlewheel porphyrin framework 5 (PPF-5) onto semiconductor surfaces modified with carboxylic acids. Using versatile diazonium and catechol chemistries to modify silicon and titania surface chemistries, we show that solvothermally grown PPF-5 selectively nucleates and grows as stacked crystalline sheets with preferential (001), (111), and (110) crystallographic orientations. Furthermore, variations in the synthesis temperature produce modified stack morphologies that correlate with changes in the surface-nucleated PPF-5 photoluminescence.

KEYWORDS: *pillared paddlewheel framework, porphyrin, metal−organic framework, surface functionalization, nucleation and growth*

■ INTRODUCTION

Metal−organic frameworks (MOFs) are porous crystalline structures formed from the highly ordered coassembly of metal cations with coordinating ligands on functional or structural organic molecules. These materials are attractive for numerous applications, including gas storage,[1,2] gas separation,[2,3] catalysis,[3,4] and sensors[2,3] because of their high surface areas and specific and tunable chemical functionalities. Fully realizing the potential utility of these versatile materials, however, requires their effective integration onto optically or electrically addressable substrates.[3,5] In the present work, the surface-nucleated, solvothermal growth of a model porphyrin-based MOF, porphyrin paddlewheel framework 5 (PPF-5), using versatile surface chemistries to mediate PPF-5 nucleation on acid-functionalized surfaces is demonstrated. PPF-5 is a member of a family of pillared MOFs containing metalloporphyrin paddlewheel linkers that introduce additional metal centers to control ligand binding and framework topology.[6] The introduction of porphyrins into these assemblies adds potentially valuable optically active or catalytic character.[7] Although porphyrin-containing MOFs have been synthesized and explored as bulk crystals[6,8−11] and their properties explored[12−14] and modified,[11,15] the solvothermal growth of these materials on functionalized semiconducting surfaces represents a new extension of this PPF-5 growth.

The controlled nucleation of MOFs on surfaces is a nontrivial endeavor, and the extent of this emerging field has been reviewed in considerable detail by Betard and Fischer.[16] Many of the approaches for growing MOF coatings on surfaces for device applications are focused on layer-by-layer deposition techniques;[7,17−20] however, straightforward approaches, such as the direct nucleation and growth of MOF crystals and thin films onto chemically functionalized substrates, remain attractive because of their simplicity and potential scalability. Reported demonstrations of solvothermal nucleation and growth of MOFs on functionalized surfaces are relatively scarce, although there has been some demonstrated success in growing MOFs such as HKUST-1 $(Cu_3(btc)_2)$,[21,22] MOF-5 $(Zn_4O(bdc))$,[23] CAU-1 $(Al_4(OH)_2(OCH_3)_4(H_2N\text{-}bdc)_3 \cdot xH_2O)$,[24] and Fe-MIL-88B[25] on gold surfaces coated with acid-terminated self-assembled monolayers (SAMs).

Here, we extend the surface functionalization concept to porphyrin paddlewheel MOFs using PPF-5 as a model compound and demonstrate nucleated growth on silicon and titanium dioxide, two technologically relevant substrates. Selective PPF-5 nucleation and growth was enabled by carboxylate surface chemistries produced using diazonium and catechol chemistries to modify silicon and titania surfaces, respectively. Without the resulting surface carboxylate groups, no PPF-5 growth occurs, showing that selective growth should

carboxyphenyl-modified Si
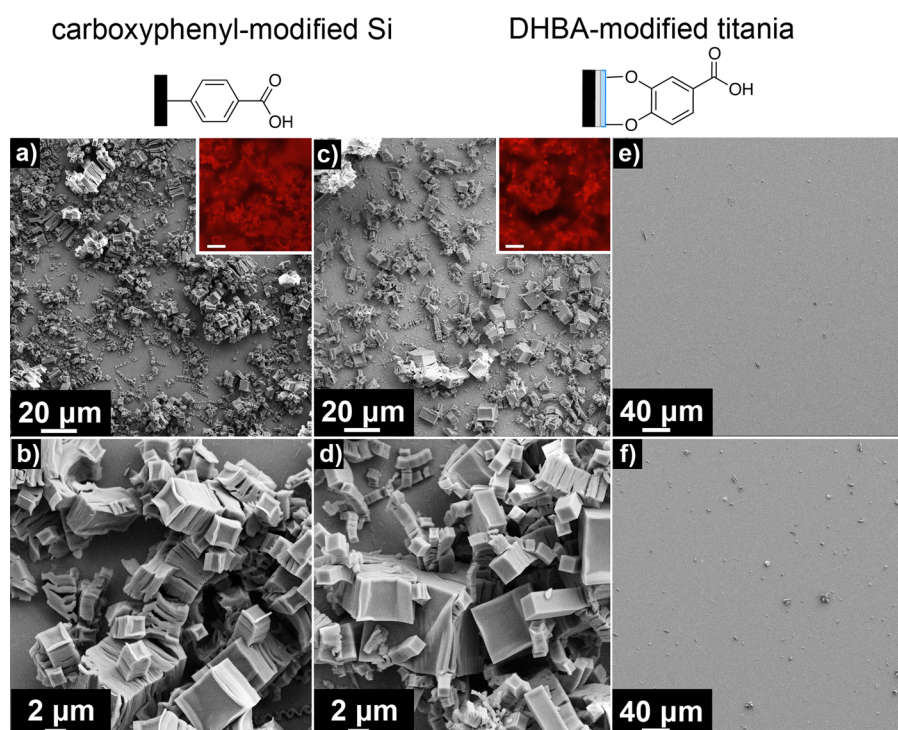
DHBA-modified titania

Figure 1. SEM images of PPF-5 crystals grown at 80 °C for 24 h onto (a and c) carboxyphenyl-functionalized Si and (b and d) DHBA-modified TiO$_2$. Control surfaces of (e) unmodified silicon and (f) unmodified titania produced no PPF-5 growth. Insets: Fluorescence images of PPF-5 crystals (λ_{ex} = 510−550 nm; scale bars correspond to 10 μm). Above: molecular schematics of the acid functionalization chemistries employed.

be feasible using a variety of surface patterning methods. These chemical approaches also expand the repertoire of surface functionalization chemistries for MOF nucleation beyond SAMs attached to gold or covalently bound using siloxane chemistry.[16] Using these alternative chemical approaches to surface modification broadens the potential applicability of MOF thin films because they allow for functionalization of a diverse range of metal,[26,27] semiconductor,[26,28,29] and oxide surfaces.[29−31] Moreover, we describe how the synthesis temperature affects the morphology of the MOF architectures and correlate the variation in morphology with changes in the optical properties of these supramolecular materials.

EXPERIMENTAL SECTION

Materials. Palladium(II) *meso*-tetrakis(4-carboxyphenyl)porphine (Pd-TCPP) was obtained from Frontier Scientific. Cobalt nitrate hexahydrate [Co(NO$_3$)$_2$·6H$_2$O], 4,4'-bipyridine (bipyridine), *N,N*-diethylformamide (DEF), 3,4-dihydroxybenzoic acid (DHBA), and phosphate-buffered saline (PBS) salts were purchased from Sigma-Aldrich and used as received.

Substrate Preparation. All silicon wafers were piranha cleaned (3:1 H$_2$SO$_4$:30% H$_2$O$_2$) prior to use or further functionalization. After piranha cleaning, silicon wafers were then immersed in a 5% hydrofluoric acid solution for at least 20 min to remove the oxide and expose the bare silicon surface. The wafers were then thoroughly rinsed with deionized water, dried with nitrogen, and used within 10 min of preparation. Modification of the silicon surfaces with *p*-carboxyphenyldiazonium tetrafluoroborate was performed according to previously published protocols.[26] The substrates were then rinsed with water and ethanol and dried with nitrogen.

Approximately 20 nm of titania was deposited onto silicon wafers using atomic layer deposition (Savannah ALD System, Cambridge Nanotech) of alternating TiCl$_4$ and H$_2$O pulses. After deposition, the titania was heated to 300 °C for 30 min in air and then ozone-treated for 10 min prior to use. DHBA functionalization was performed by immersion in a 10 mM solution of DHBA in pH 7 PBS for 2 h. The

substrates were then washed in deionized water and dried with nitrogen.

PPF-5 Synthesis. Synthesis of PPF-5 crystals was performed using a previously published method.[6] In a typical synthesis, a substrate was inserted vertically into a solution consisting of 9.2 mg (0.01 mmol) of Pd-TCPP, 8.8 mg (0.03 mmol) of Co(NO$_3$)$_2$·6H$_2$O, and 2.8 mg (0.01 mmol) of bipyridine dissolved in a solvent mixture containing 1.5 mL of DEF and 0.5 mL of ethanol. This solution was then heated to 60, 80, or 100 °C for 24 h. After growth, the samples were removed from the growth solution and rinsed with DEF and ethanol to remove remnant reagent and any sedimented PPF-5 crystals.

Characterization. Static contact-angle measurements were collected on a Kruss DSA Mk1 Instrument. Scanning electron microscopy (SEM) analysis was performed on a Zeiss Supra 55VP field-emission scanning electron microscope. Microphotoluminescence was collected during fluorescence imaging under green band excitation (510−550 nm) and collection of light with wavelengths longer than 590 nm on an optical microscope fitted with a spectrometer. A Siemens model D500 $\theta-2\theta$ powder diffractometer (Bruker AXS, Inc., Madison, WI) was used for grazing-incidence X-ray diffraction (GIXRD) data collection with samples maintained at room temperature (25 °C). Monochromatic Cu Kα (λ = 0.15406 nm) radiation was produced using a diffracted-beam curved graphite monochromator. Fixed 0.3° incident beam and scatter slits were used (goniometer radius = 120 mm), and the instrument power settings were 40 kV and 30 mA. *Datascan V4.3* (Materials Data Inc., Livermore, CA) software was used to operate the diffractometer. Powder X-ray diffraction (XRD) patterns were collected using a fixed q angle of 1°, and scans were collected as follows: 2−40° 2θ range, step size of 0.04° 2θ, and a count time of 1 s. Each PPF-5 sample (grown on a silicon substrate) was drawn directly out of the solvent solution, mounted on an XRD sample holder within 1 min, and subsequently loaded onto a diffractometer for XRD analysis. Diffraction patterns were collected with a thin layer of DEF covering the surface to prevent structural collapse of the MOF due to drying effects. X-ray photoelectron spectroscopy (XPS) was performed with a Kratos Axis Ultra DLD instrument with base pressures of less than 5 × 10^{-9} Torr. A

1510

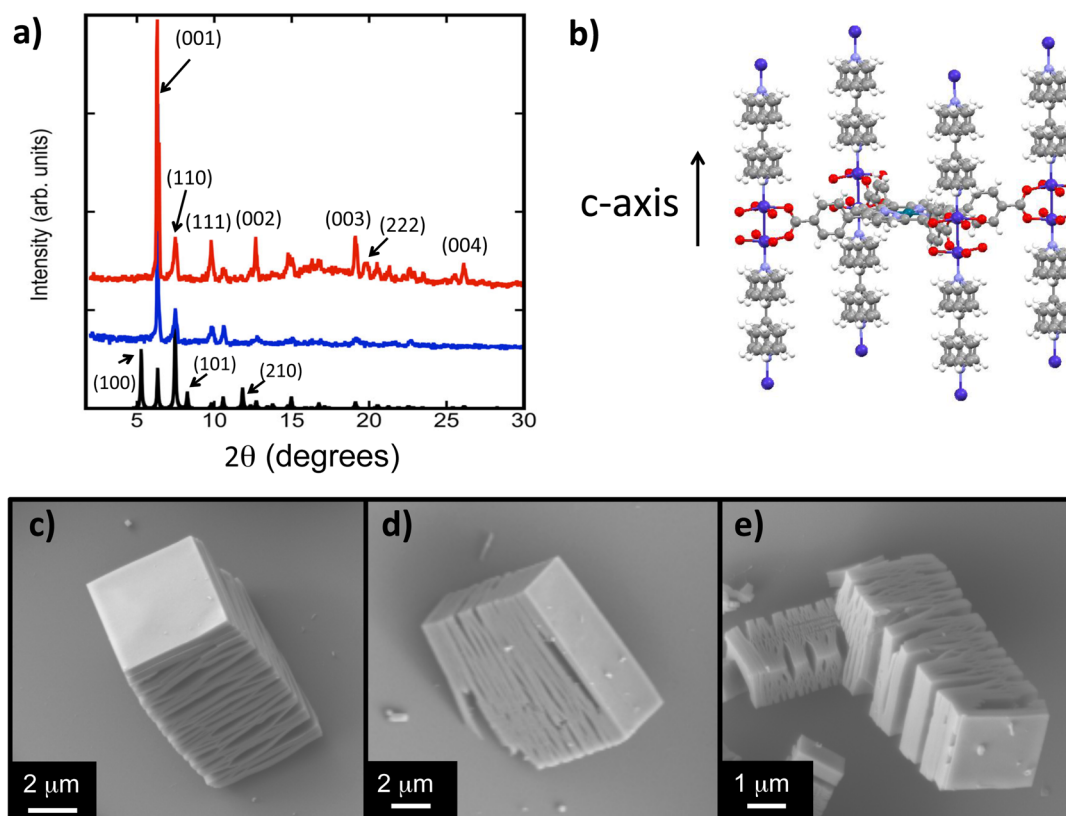dx.doi.org/10.1021/am404102f | ACS Appl. Mater. Interfaces 2014, 6, 1509−1514

Figure 2. (a) GIXRD patterns for PPF-5 grown on carboxyphenyl-modified silicon (blue) and DHBA-modified titania (red) shown with the calculated pattern for PPF-5 (black). Strong or enhanced reflections are labeled above, while peaks absent in the measured data are indicated on the calculated pattern below. (b) Schematic PPF-5 crystal structure and c-axis orientation. Dark blue spheres are cobalt, red spheres are oxygen, lavender spheres are nitrogen, gray spheres are carbon, white spheres are hydrogen, and the green sphere is palladium. (c−e) SEM images of PPF-5 crystals grown at 80 °C on DHBA-modified titania, with the vertical stack growing along the [001] direction (c), the [111] direction (d), and both the [110] and [111] directions (e).

monochromatic Al Kα (1486.7 eV) source was used at 300 W. The analyzer was used in hybrid mode with a pass energy of 160 eV for survey spectra and 20 eV for high-resolution spectra. The analysis area was an elliptical 300 × 700 μm for each sample. Survey spectra were taken with 1000 meV step sizes and 100 ms dwell times. The C 1s peaks were recorded with 30 meV step sizes and 100 ms dwell times. Data processing was performed with *CasaXPS*. C 1s peak fitting was performed with a Shirley background and Gaussian/Lorentzian (70/30) peaks.

■ RESULTS AND DISCUSSION

PPF-5 consists of planes of carboxylic acid-decorated palladium-containing metalloporphyrins coordinated to Co^{2+} and bipyridine pillars linking parallel planes. Because PPF-5 contains metal ions coordinated to electron-donating and/or anionic groups, we hypothesize that acid-decorated surfaces will promote nucleation and growth of MOFs containing these functional groups on their linkers.[3] In this work, we examine the effects of carboxylic acid functionalities on the nucleation and growth of PPF-5 on both silicon and titania surfaces. Silicon was modified with *p*-carboxyphenyldiazonium tetrafluoroborate. Titania, deposited by atomic layer deposition on silicon wafers, was functionalized using DHBA. Effective surface modification was verified by contact-angle measurements (Table S1 in the SI). The presence of carboxylic acid moieties on these functionalized surfaces was confirmed by XPS, determined by examination of the C 1s spectra. In addition to the major XPS peak at 284.6 eV expected for the C−C environment in these samples, the XPS spectra revealed peaks

at 288.7 and 288.8 eV for the DHBA-modified titania and carboxyphenyl-modified silicon, respectively, indicating the presence of carboxylic acids.[32−34] Deconvoluted XPS spectra taken from these samples may be seen in the SI (Figure S2).

Heterogeneous nucleation and growth of PPF-5 was performed on vertically oriented substrates immersed within a reagent solution for solvothermal crystal growth. Figure 1 shows SEM images of PPF-5 crystals grown at 80 °C for 24 h onto carboxyphenyl-modified silicon (a and b) and DHBA-modified titania (c and d). On both substrates, crystals grown at 80 °C appeared as stacks of rectangular plates. Although the majority of crystals were nucleated directly on the substrate surfaces, there was some evidence of secondary crystal nucleation off existing crystals. The dimensions of these plates vary from ca. 1 μm^2 to ca. 100 μm^2, while the height of the stacks approaches ca. 3−5 μm. In contrast to the acid-modified surfaces, unmodified silicon and titania surfaces (Figure 1e,f) show no significant PPF-5 crystal growth. Fluorescence emission is also observed throughout the PPF-5 crystals, as seen in the fluorescence microscope image insets of Figure 1a,c, which verifies the incorporation of a photoactive palladium-containing metalloporphyrin throughout the crystals. That the PPF-5 growth is selective for the modified surfaces and that pronounced crystal growth is observed on two different substrate types, with each acid functionalized with different chemistries, provide strong evidence for the acid-mediated nucleation and growth of PPF-5.

1511

dx.doi.org/10.1021/am404102f | *ACS Appl. Mater. Interfaces* 2014, 6, 1509−1514

Figure 2a presents GIXRD patterns for PPF-5 grown for 24 h on carboxyphenyl-modified silicon (blue) and DHBA-modified titania (red) compared to the pattern calculated for unoriented (i.e., random) PPF-5 (black). Figure 2b contains a schematic of the PPF-5 crystal structure, in which the c axis is parallel to the vertical bipyridine pillars, while the ab plane is defined by the horizontal porphyrin linking the bipyridine pillars. The patterns for PPF-5 grown on the carboxylic acid-modified substrates match well with the calculated XRD pattern for the tetragonal PPF-5,[6] verifying that heterogeneous nucleation and growth of PPF-5 is occurring during solvothermal synthesis. Careful examination of these diffraction patterns, however, reveals notable crystallographic orientation of PPF-5. In the patterns taken of PPF-5 grown on DHBA-modified titania, and to a lesser degree for PPF-5 on carboxy-modified silicon, there are strong (110) reflections and the (001), (111), (002), (003), (222), and (004) reflections appear significantly enhanced, relative to the calculated pattern shown in black. Interestingly, the (100), (101), and (210) reflections are not observed or are strongly suppressed on both sample substrates as well. These observations indicate preferential growth of PPF-5 along the [001], [110], and [111] directions. The SEM images in Figure 2c−e show remarkable examples of PPF-5 nanostacks growing along these preferred [001], [111], and [110]/[111] directions, respectively. Upon interpretation of these images, it is reasonably assumed that the crystal structure correlates with the morphology of the nanostacks, such that the porphyrin-containing ab plane lies parallel to the plane of the sheets in the nanostacks. The lower magnification images in Figure 1 show a polycrystalline composite of nanostacks with these crystal orientations, although it should be noted that a portion of the relatively jumbled appearance of these crystals may be attributed to crystal stacks that have either broken and fallen or simply tilted over during drying (in preparation for SEM). The flexibility of the largely organic sheets may also contribute to tilting or bending of the stacks, as well as the apparently loose packing of the sheets in the stacks (Figure 2c−e).

In previous reports, other MOFs grown on carboxylate-rich SAM-coated surfaces have been shown to induce oriented crystal growth.[19,21,35] In previously reported cases, the demonstrated heterogeneous nucleation and growth of MOFs involves using surface-bound coordinating ligands to bind the metal cations of the MOF, forming a molecular seed layer capable of promoting subsequent MOF crystallization.[3] In the present system, we expect that surface-functionalized carboxylate binding concentrates Co^{2+} on the substrate surface, providing a metal-rich environment to seed the binding of the bipyridine pillars or porphyrins. We speculate that how the porphyrins, bipyridine molecules, and Co^{2+} ions cooperatively interact and bind to the acid-modified surfaces determines the crystallographic selectivity observed in this system. For example, porphyrins binding horizontally on an acidic surface enriched with Co^{2+} ions would be expected to promote preferential vertical crystal growth along the observed [001] direction. Alternatively, growth along directions such as [100], a direction not observed in the diffraction in Figure 2a, would be selected against in this system because this would require nucleation on the unlikely configuration of multiple bipyridines bound to the functionalized surface, oriented parallel to each other and separated exactly 1 unit cell apart. The exact mechanisms responsible for the observed preferential crystal growth are likely complex, and it is not the intention of this paper to discuss those mechanisms in detail. Still, it is apparent

from the observations presented here that the acid-functionalized surface not only promotes crystal nucleation but also influences the crystallographic orientation of the nucleating PPF-5 crystal nanostacks.

Interestingly, when the PPF-5 growth temperature is increased to 100 °C, the morphology of PPF-5 crystals changes. The SEM images in Figure 3 show structures typical
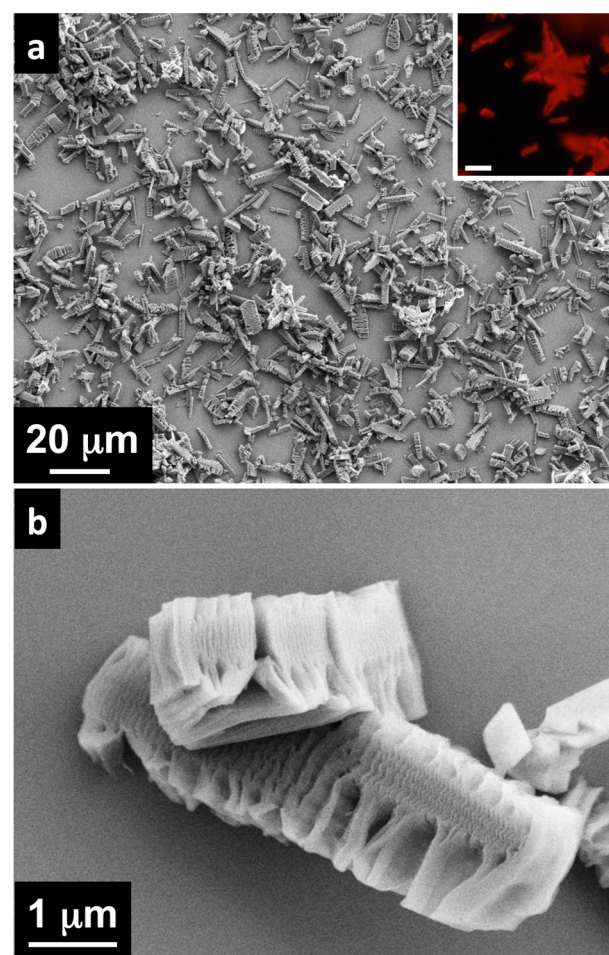

Figure 3. SEM images of PPF-5 grown for 24 h at 100 °C on carboxyphenyl-modified silicon. Inset: Fluorescence image of PPF-5 crystals (scale bars correspond to 10 μm).

of those seen on both carboxyphenyl-modified silicon and DHBA-modified titania. These structures still form as stacks of PPF-5 sheets, but at the center of the structures, fine sheets pack together to create a dense, corrugated core. Extending from this core are more coarse, ribbonlike sheets packed much less densely together. Fluorescence imaging (Figure 3a inset) shows uniform fluorescence from the PPF-5 crystals, indicating that the palladium-containing metalloporphyrin is present throughout both low- and high-density regions of the crystals, and GIXRD confirms that PPF-5 grown at 100 °C exhibits the same orientational preference as that displayed at 80 °C. The synthetic mechanisms responsible for the dual morphology in these materials are not clear at this time, but we postulate that these structures may have formed in a two-stage growth process in which rapid initial crystal nucleation to form the dense core is followed by a steady-state growth phase that produces the more coarse, loosely packed sheets.

Controlling the crystal size and nanoscale morphology is important to regulating the properties and functions of MOFs. In some instances, this control can be achieved by incorporating additives during crystal growth.[36−40] Alternatively, Stavila et al.[35] recently showed that the film morphology and roughness of HKUST-1 can be influenced by the composition of the substrate, with smoother films produced on silica substrates than on alumina. The present work indicates that surface-nucleated PPF-5 crystal morphology can be tuned simply by controlling the growth temperature.

As an illustration of how the nanoscale morphology of these surface-nucleated MOFs may influence macroscopic properties, changes in the optical response of the photoactive PPF-5 structures were explored. Figure 4 illustrates how the
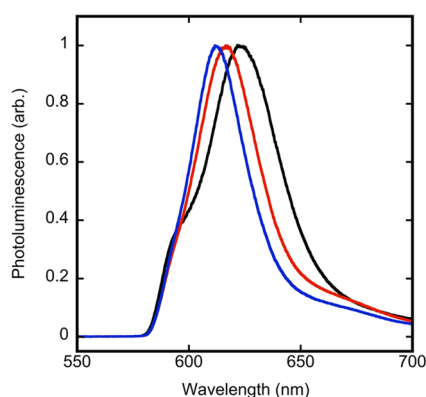

Figure 4. Fluorescence emission spectra for PPF-5 crystals grown on carboxyphenyl-functionalized silicon substrates at 80 (red) and 100 °C (blue) compared to Pd-TCPP (black).

photoluminescence (broad excitation between 510 and 550 nm) for PPF-5 crystals grown on carboxyphenyl-functionalized silicon can be influenced by the growth temperature and associated morphology change. The black curve shows the photoluminesence of the palladium metalloporphyrin, the primary luminescent species in these MOFs. This spectrum shows a maximum emission at 622 nm and a shoulder just below 600 nm. When this porphyrin is incorporated into the crystalline environment of PPF-5, the shoulder disappears, and the maximum emission blue-shifts. Crystals prepared at 80 °C show a blue shift of the maximum to 617 nm, while a further shift to 612 nm is observed for crystals grown at 100 °C. The molecular environment surrounding the porphyrins in the more densely packed structures created at 100 °C appears to have further blue-shifted the photoluminescent emission. Although this is a relatively subtle change, it is, nonetheless, easily measured and is, to our knowledge, the first example of a microstructure-induced change in a MOF optical property.

CONCLUSIONS

The heterogeneous solvothermal crystal growth of PPF-5 was explored on silicon and titania surfaces modified with widely applicable chemistries: *p*-carboxyphenyldiazonium tetrafluoroborate and DHBA. Vertical PPF-5 stacks of rectangular sheets, showing preferential (001), (110), and (111) crystallographic orientation, grew selectively on acid-modified surfaces. The crystal size, morphology, and density were nominally identical for both surface modification approaches. Furthermore, the morphology of PPF-5 crystals grown on these modified surfaces was demonstrated to be thermally tunable because increasing

the crystal growth temperature influenced the morphology of the structures, producing PPF-5 stacks with a densely packed core connected to a loosely packed stack exterior. This change in the morphology was correlated with a blue shift in the photoluminescence, revealing tunable variation not only of the structure but also of the properties. This demonstration of surface-induced growth of an optically active porphyrin paddlewheel framework on semiconducting surfaces may enable broader applicability of these functional materials in emerging optoelectronic systems.

ASSOCIATED CONTENT

S **Supporting Information**
Schematics depicting surface functionalization of titania and silicon, measured static contact angles from these surfaces, and plots of deconvoluted XPS data used to identify carboxylic acid funtionalization of titania and silicon surfaces. This material is available free of charge via the Internet at http://pubs.acs.org.

AUTHOR INFORMATION

Corresponding Author
*E-mail: edspoer@sandia.gov. Tel.: (505) 284-1932.

Author Contributions
The manuscript was written through contributions of all authors. All authors have given approval to the final version of the manuscript.

Notes
The authors declare no competing financial interest.

ACKNOWLEDGMENTS

REFERENCES

(1) Sumida, K.; Rogow, D. L.; Mason, J. A.; McDonald, T. M.; Bloch, E. D.; Herm, Z. R.; Bae, T. H.; Long, J. R. *Chem. Rev.* **2012**, *112*, 724−781.
(2) Kreno, L. E.; Leong, K.; Farha, O. K.; Allendorf, M.; Van Duyne, R. P.; Hupp, J. T. *Chem. Rev.* **2012**, *112*, 1105−1125.
(3) Shekhah, O.; Liu, J.; Fischer, R. A.; Woll, C. *Chem. Soc. Rev.* **2011**, *40*, 1081−1106.
(4) Lee, J.; Farha, O. K.; Roberts, J.; Scheidt, K. A.; Nguyen, S. T.; Hupp, J. T. *Chem. Soc. Rev.* **2009**, *38*, 1450−1459.
(5) Allendorf, M. D.; Schwartzberg, A.; Stavila, V.; Talin, A. A. *Chem.—Eur. J.* **2011**, *17*, 11372−11388.
(6) Choi, E. Y.; Barron, P. M.; Novotny, R. W.; Son, H. T.; Hu, C. H.; Choe, W. *Inorg. Chem.* **2009**, *48*, 426−428.
(7) Makiura, R.; Kitagawa, H. *Eur. J. Inorg. Chem.* **2010**, 3715−3724.
(8) Abrahams, B. F.; Hoskins, B. F.; Michail, D. M.; Robson, R. *Nature* **1994**, *369*, 727−729.
(9) Goldberg, I. *Chem. Commun.* **2005**, 1243−1254.
(10) Farha, O. K.; Shultz, A. M.; Sarjeant, A. A.; Nguyen, S. T.; Hupp, J. T. *J. Am. Chem. Soc.* **2011**, *133*, 5652−5655.

(11) Wang, X. S.; Meng, L.; Cheng, Q. G.; Kim, C.; Wojtas, L.; Chrzanowski, M.; Chen, Y. S.; Zhang, X. P.; Mat, S. Q. *J. Am. Chem. Soc.* **2011**, *133*, 16322−16325.

(12) Kosal, M. E.; Chou, J. H.; Wilson, S. R.; Suslick, K. S. *Nat. Mater.* **2002**, *1*, 118−121.

(13) Shultz, A. M.; Farha, O. K.; Hupp, J. T.; Nguyen, S. T. *J. Am. Chem. Soc.* **2009**, *131*, 4204−+.

(14) Son, H. J.; Jin, S. Y.; Patwardhan, S.; Wezenberg, S. J.; Jeong, N. C.; So, M.; Wilmer, C. E.; Sarjeant, A. A.; Schatz, G. C.; Snurr, R. Q.; Farha, O. K.; Wiederrecht, G. P.; Hupp, J. T. *J. Am. Chem. Soc.* **2013**, *135*, 862−869.

(15) Matsunaga, S.; Endo, N.; Mori, W. *Eur. J. Inorg. Chem.* **2011**, 4550−4557.

(16) Betard, A.; Fischer, R. A. *Chem. Rev.* **2012**, *112*, 1055−1083.

(17) Motoyama, S.; Makiura, R.; Sakata, O.; Kitagawa, H. *J. Am. Chem. Soc.* **2011**, *133*, 5640−5643.

(18) Shekhah, O.; Wang, H.; Paradinas, M.; Ocal, C.; Schupbach, B.; Terfort, A.; Zacher, D.; Fischer, R. A.; Woll, C. *Nat. Mater.* **2009**, *8*, 481−484.

(19) Shekhah, O.; Wang, H.; Kowarik, S.; Schreiber, F.; Paulus, M.; Tolan, M.; Sternemann, C.; Evers, F.; Zacher, D.; Fischer, R. A.; Woll, C. *J. Am. Chem. Soc.* **2007**, *129*, 15118−+.

(20) Zacher, D.; Schmid, R.; Woll, C.; Fischer, R. A. *Angew. Chem., Int. Ed.* **2011**, *50*, 176−199.

(21) Biemmi, E.; Scherb, C.; Bein, T. *J. Am. Chem. Soc.* **2007**, *129*, 8054−+.

(22) Zhuang, J.-L.; Ceglarek, D.; Pethuraj, S.; Terfort, A. *Adv. Funct. Mater.* **2011**, *21*, 1442−1447.

(23) Hermes, S.; Schroder, F.; Chelmowski, R.; Woll, C.; Fischer, R. A. *J. Am. Chem. Soc.* **2005**, *127*, 13744−13745.

(24) Hinterholzinger, F.; Scherb, C.; Ahnfeldt, T.; Stock, N.; Bein, T. *Phys. Chem. Chem. Phys.* **2010**, *12*, 4515−4520.

(25) Scherb, C.; Schodel, A.; Bein, T. *Angew. Chem., Int. Ed.* **2008**, *47*, 5777−5779.

(26) Stewart, M. P.; Maya, F.; Kosynkin, D. V.; Dirk, S. M.; Stapleton, J. J.; McGuiness, C. L.; Allara, D. L.; Tour, J. M. *J. Am. Chem. Soc.* **2004**, *126*, 370−378.

(27) Dalsin, J. L.; Hu, B. H.; Lee, B. P.; Messersmith, P. B. *J. Am. Chem. Soc.* **2003**, *125*, 4253−4258.

(28) deVilleneuve, C. H.; Pinson, J.; Bernard, M. C.; Allongue, P. *J. Phys. Chem. B* **1997**, *101*, 2415−2420.

(29) Rice, C. R.; Ward, M. D.; Nazeeruddin, M. K.; Gratzel, M. *New J. Chem.* **2000**, *24*, 651−652.

(30) Rodriguez, R.; Blesa, M. A.; Regazzoni, A. E. *J. Colloid Interface Sci.* **1996**, *177*, 122−131.

(31) Ting, G. G.; Acton, O.; Ma, H.; Ka, J. W.; Jen, A. K. Y. *Langmuir* **2009**, *25*, 2140−2147.

(32) Han, S.; Joo, S.; Ha, T.; Kim, Y.; Kim, K. *J. Phys. Chem. B* **2000**, *104*, 11987−11995.

(33) Schnadt, J.; O'Shea, J.; Patthey, L.; Schiessling, J.; Krempasky, J.; Shi, M.; Martensson, N.; Bruehwiler, P. *Surf. Sci.* **2003**, *544*, 74−86.

(34) Wells, M.; Dermody, D.; Yang, H.; Kim, T.; Crooks, R. *Langmuir* **1996**, *12*, 1989−1996.

(35) Stavila, V.; Volponi, J.; Katzenmeyer, A. M.; Dixon, M. C.; Allendorf, M. D. *Chem. Sci.* **2012**, *3*, 1531−1540.

(36) Li, Y. S.; Bux, H.; Feldhoff, A.; Li, G. L.; Yang, W. S.; Caro, J. *Adv. Mater.* **2010**, *22*, 3322−+.

(37) Pham, M. H.; Vuong, G. T.; Fontaine, F. G.; Do, T. O. *Cryst. Growth Des.* **2012**, *12*, 3091−3095.

(38) Umemura, A.; Diring, S.; Furukawa, S.; Uehara, H.; Tsuruoka, T.; Kitagawa, S. *J. Am. Chem. Soc.* **2011**, *133*, 15506−15513.

(39) Pham, M. H.; Vuong, T.; Vu, A. T.; Do, T. O. *Langmuir* **2011**, *27*, 15261−15267.

(40) McCarthy, M. C.; Varela-Guerrero, V.; Barnett, G. V.; Jeong, H. K. *Langmuir* **2010**, *26*, 14636−14641.